JOURNAL OF GEOPHYSICAL RESEARCH, VOL. 99, NO. D5, PAGES 10,823–10,831, MAY 20, 1994

Possible implications of global climate change on global lightning distributions and frequencies

Colin Price[1] and David Rind

NASA Goddard Institute for Space Studies, Columbia University, New York

Abstract. The Goddard Institute for Space Studies (GISS) general circulation model (GCM) is used to study the possible implications of past and future climate change on global lightning frequencies. Two climate change experiments were conducted: one for a 2 × CO_2 climate (representing a 4.2°C global warming) and one for a 2% decrease in the solar constant (representing a 5.9°C global cooling). The results suggest a 30% increase in global lightning activity for the warmer climate and a 24% decrease in global lightning activity for the colder climate. This implies an approximate 5–6% change in global lightning frequencies for every 1°C global warming/cooling. Both intracloud and cloud-to-ground frequencies are modeled, with cloud-to-ground lightning frequencies showing larger sensitivity to climate change than intracloud frequencies. The magnitude of the modeled lightning changes depends on season, location, and even time of day.

Introduction

There is a growing amount of evidence that present-day trends in atmospheric trace gas concentrations will result in a global warming of 1.5°–4.5°C by the middle of the twenty-first century [*Intergovernmental Panel on Climate Change (IPCC)*, 1990]. One possible impact of this warming could be on the frequency and intensity of thunderstorms. Since tropical thunderstorms and deep convection are directly linked to the transport of momentum, heat, and moisture in the atmosphere, changes in global thunderstorm frequencies and intensities could possibly influence the general circulation of the atmosphere.

One aspect of thunderstorms is lightning activity. Lightning frequencies in thunderstorms supply useful information regarding the dynamics and microphysics of convective storms. Lightning flash rate is related to the stage of convective cloud development [*Williams et al.*, 1989], the intensity of updrafts [*Lhermitte and Williams*, 1983], cloud liquid water content [*Saunders et al.*, 1991], cloud structure [*Rust and Doviak*, 1982], and even convective precipitation volume [*Buechler et al.*, 1990].

Lightning is also of interest in other fields of research. It is known that lightning is a major source of NO_x in the atmosphere [*Franzblau and Popp*, 1989], which can influence concentrations of O_3 both in the troposphere and in the stratosphere. Although lightning activity is concentrated mainly in the tropics, lightning is a major cause of natural forest fires in midlatitudes. In the United States alone, more than 10,000 fires occur every year as a result of lightning [*U.S. Department of Agriculture (USDA) Forest Service*, 1992]. On the human side, lightning is a major cause of weather-related deaths, property damage, and interference with power system operations.

If the frequency of lightning activity changes as a result of future climate change, there may be major ramifications for all lightning-related phenomena. In this study a climate model is used to investigate the possible implications of global climate change on global lightning frequencies.

Model

The global model used in this study is the Goddard Institute for Space Studies (GISS) general circulation model (GCM). The Model II version has a horizontal resolution of 8° × 10°, with nine layers in the vertical: two in the boundary layer, five or six in the troposphere, and one or two in the stratosphere (depending upon latitude). The model is described extensively by *Hansen et al.* [1983].

The global lightning distributions are calculated using the model's moist convection parameterization. The GISS model uses a penetrative convective scheme based on parcel theory [*DelGenio and McGrattan*, 1990]. It is assumed that somewhere within the 8° × 10° grid box, conditions are favorable to lift a parcel of air into the grid box above. This could be a result of either temperature or moisture fluctuations on the subgrid scale. Convection is then triggered if the moist static energy of the lower layer exceeds the saturation moist static energy of the layer above and the implied lifting produces saturation; this defines the cloud base. An arbitrary 50% of the mass of the cloud base grid box rises in each event. The cloud top occurs at the top of the highest layer for which vertical mass flux, due to moist convection, occurs. This implies that overshooting into the stratosphere is possible. Latent heat release serves to maintain cloud buoyancy, and heating/cooling of the environment takes place via compensating environmental subsidence, detrainment of cloud air at cloud top, and evaporation of falling condensate. Condensed water is not transported upward but is allowed to reevaporate into 25% of each lower layer above cloud base and 50% below; the remainder determines the convective precipitation. The convective plume and subsiding environment transport grid-scale horizontal momentum. All types of convection are predicted by the same criteria; differentiation

[1]Now at Global Climate Research Division, Lawrence Livermore National Laboratory, Livermore, California.

Paper number 94JD00019.
0148-0227/94/94JD-00019$05.00

between deep and shallow depends only on the cloud buoyancy constraint.

The lightning parameterizations have been developed and described by *Price and Rind* [1992, 1993]. For total lightning frequencies, two formulations are used: one for continental thunderstorms and one for oceanic thunderstorms, both using convective cloud top height as the predictive variable. The continental parameterization is based on observations showing that lightning frequencies in continental thunderstorms are related to the fifth power of the cloud height [*Shackford*, 1960; *Jacobson and Krider*, 1976; *Livingston and Krider*, 1978; *Williams*, 1981, 1985]. The parameterization for marine thunderstorms is based on observations showing marine thunderstorms with very weak updraft intensities [*Jorgensen and LeMone*, 1989], resulting in extremely low lightning frequencies [*Takahashi*, 1990]. The relationships used are

$$F_c = 3.44 \times 10^{-5} H^{4.90}$$

$$F_m = 6.40 \times 10^{-4} H^{1.73}$$

where $F_{c,m}$ is lightning frequency for continental and marine thunderstorms (flashes/minute) and H is cloud top height above ground (kilometers).

To calculate the cloud-to-ground lightning frequencies, the proportion of cloud-to-ground flashes in a thunderstorm is related to the thickness of the cold cloud sector (0°C level to cloud top) [*Price and Rind*, 1993]. As the mixed phase region within the cold cloud sector expands as a cloud develops, the probability of dielectric breakdown increases due to increases in the electric field strength. This results in an increase in intracloud lightning discharges, or a decrease in the fraction of cloud-to-ground discharges in the thunderstorm. Therefore as the thickness of the cold cloud sector increases, the fraction of cloud-to-ground flashes decreases [*Rutledge et al.*, 1992; *Price and Rind*, 1993]. This also implies that in tropical regions, where the depth of thunderstorms above the freezing level is generally large, the proportion of cloud-to-ground flashes in thunderstorms is less than in midlatitudes. The empirically derived formulation used in the GCM to determine the proportion of cloud-to-ground flashes (P) in an individual thunderstorm is

$$P = (aD^4 + bD^3 + cD^2 + dD + e)^{-1}$$

where $a = 0.021$, $b = -0.648$, $c = 7.49$, $d = -36.54$, $e = 64.09$, and D is cold cloud thickness (kilometers).

The GISS GCM has a time step of 1 hour for the moist convective scheme and 15 min for the large-scale dynamics. The model's spin-up time for each climate change experiment is approximately 25 model years, after which the ocean's mixed layer temperatures have reached equilibrium. The model continues to run through year 35, and the climatological diagnostics are obtained from the mean of the last 10 years of the run (year 25 through 35).

Before any climate change experiments can be done, it is first necessary to determine how well the model can simulate current lightning distributions. The analysis of the model's control climate is extensively presented by *Price and Rind* [1994]. The model's control run gives an annual mean global lightning frequency of 77 flashes/s, of which 25% is cloud-to-ground lightning. The model's global lightning spatial distribution shows an 89% agreement with observed global lightning distributions [*Turman and Edgar*, 1982]. When comparing the model's flash rates with observed global values, a correlation coefficient of approximately 0.50 is obtained, which is highly significant at the 99.9% level. The GCM's annual, seasonal, and diurnal variations for the control climate show good agreement with the observations [*Price and Rind*, 1994].

Climate Change Experiments

To investigate the sensitivity of lightning frequencies to climate change we consider two climate change scenarios. The first is for a climate with twice the present-day concentration of atmospheric CO_2, i.e., 630 ppm ($2 \times CO_2$ from now on). After doubling the CO_2 concentration in the model, the surface temperatures need to restabilize. At equilibrium the global mean surface temperatures are 4.2°C warmer than in the control run. This is within the range of the predicted warming for the twenty-first century. The second experiment involves reducing the solar irradiance by 2% (-2% S_0 from now on). In this experiment the equilibrium global mean surface temperatures are 5.9°C colder than in the control run. This is approximately equivalent to the probable surface cooling at the peak of the last ice age (18,000 B.P.).

The vertical gradient of moist static energy, the sum of sensible heat, latent heat, and geopotential energy is a useful indicator of the likelihood and intensity of deep convective storms. High values of moist static energy near the surface, relative to the air above, and high relative humidity favor deep penetrating convection and the development of thunderstorms. Figure 1a shows the global mean vertical profile of moist static energy for the control climate and for the two climate change experiments. As the climate warms/cools, the maximum increase/decrease of moist static energy occurs near the surface (Figure 1b), because of the higher/lower absolute humidity associated with increased/decreased evaporation, increasing/decreasing the latent energy in the boundary layer. Secondary maxima occur in the upper troposphere since this is the level of maximum warming/cooling in the two scenarios, increasing/decreasing the sensible energy at this level. For the warmer climate the increase in the global mean surface moist static energy is approximately 2 KJ/kg larger than that at higher altitudes, which represents a 47% enhancement of the boundary layer gradient of moist static energy. For the colder climate the global mean surface moist static energy decreases by approximately 2.5 KJ/kg more than at higher altitudes, representing an 80% decrease in the boundary layer gradient of moist static energy.

The vertical mass exchange due to deep moist convection increases/decreases in a warmer/colder climate. The global average depth of penetration by all moist convective clouds (dP) changes by +17 mbar/−16 mbar for the warmer/colder climates, from dP = 395 mbar in the control climate, to dP = 412 mbar/379 mbar in the $2 \times CO_2$/-2% S_0 experiments. The implication from these changes is that the warmer/colder climate is prone to more/less intense thunderstorms and hence lightning activity.

Annual Mean Changes

The annual mean changes in total lightning frequencies, relative to the control run, for the warmer and colder climates are presented in Plate 1. In Plate 1a the changes in surface temperature for the two climate change experiments

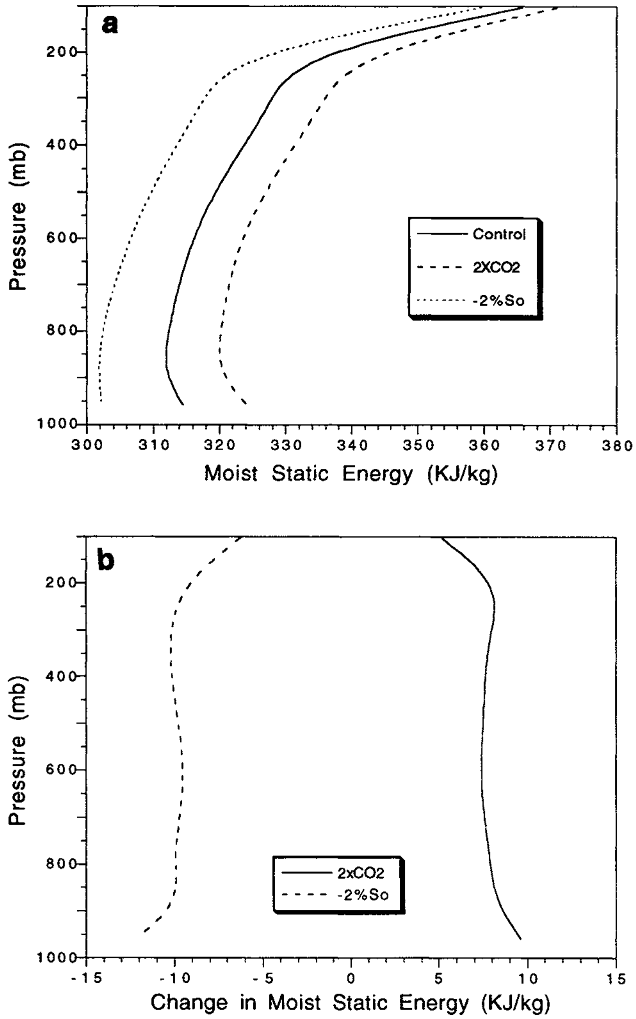

Figure 1. (a) Global mean profile of moist static energy for the three climate runs: control, 2 × CO_2, and −2% S_0. (b) Change in global mean moist static energy in the 2 × CO_2 and −2% S_0 experiments, relative to the control run.

are presented. Increases/decreases in temperature are shown in red/blue. Because of the snow/ice albedo feedback [*Hansen et al.*, 1984], higher latitudes experience more warming/cooling than lower latitudes. Plate 1b shows the absolute change in lightning frequencies for the two experiments. Increases/decreases in lightning frequencies in the warmer/cooler climate are represented by the red/blue shadings. It is clear that the largest increases/decreases occur in the tropical continental regions, where the majority of lightning occurs in the present climate. Some decreases/increases do occur in the warmer/cooler climate as a result of increased/decreased large-scale subsidence in subtropical regions resulting from the increased/decreased intensity of tropical convection.

Although the absolute increases/decreases in lightning frequencies are largest in the tropics, the percentage increases/decreases in flash rates is fairly uniform at all latitudes (Plate 1c). Small absolute changes at high latitudes represent large percentage changes, which can often be important. For example, on a global scale, Alaska receives a small fraction of lightning every year. However, this lightning has a dramatic effect on the number of lightning-caused forest fires in Alaska [*USDA Forest Service*, 1992]. A small absolute increase on a global scale is translated to a large percentage increase. A 100% increase in the frequency of lightning in high latitudes could have a dramatic influence on the frequency of forest fires in those regions.

The annual mean change for the warmer/colder climate is +30%/−24%. This implies an approximate 5–6% change in lightning frequencies for every 1°C of global warming or cooling. This sensitivity to global temperatures is similar to that obtained when fluctuations in a global lightning index were correlated with observed global surface temperature fluctuations [*Price*, 1993]. The observations showed that a 1°C increase in global surface temperatures could possibly result in an approximate 7% increase in both global lightning activity and ionospheric potential. This observed sensitivity may be different when considering a surface cooling.

Although the above global mean changes are smaller than 30%, certain locations show changes greater than 100%. In addition, the majority of changes occur where lightning activity occurs today, i.e., over continental regions. In fact, globally, lightning activity over continental regions (grid boxes with more than 50% land) changes by +72%/−45% for the two experiments, whereas over the oceans, lightning activity changes by only +12%/−15%.

Seasonal Changes

There is a significant difference between the seasonal cycle of lightning activity in the tropics and that observed globally. There is evidence that tropical regions indicate a semiannual cycle with maximum lightning activity occurring during the spring and autumn [*Williams*, 1994]. However, when extratropical storms are included, the semiannual cycle of lightning is greatly reduced and a broad maximum appears during the northern hemisphere summer [*Krumm*, 1962; *Trent and Gathman*, 1972]. This is apparently due to the presence of larger areas of landmasses in northern hemisphere midlatitudes compared with the southern hemisphere. These different seasonal cycles are reproduced by the GCM (Figures 2a and 2b), although the spring maximum in the semiannual cycle appears to be stronger than the autumn maximum. The changes in the seasonal cycles are also presented in Figure 2 for the two climate change scenarios.

Globally, as the climate warms, the model indicates that the global seasonal cycle intensifies, while the maximum lightning activity shifts from August in the colder climate to June in the warmer climate. In the tropics the semiannual cycle appears to be eroded as the climate warms. The cold climate has the best defined semiannual cycle. This erosion of the semiannual cycle is a result of the model's maximum increase in lightning activity occurring during the northern hemisphere summer, resulting in a decrease in the amplitude of the semiannual signal. For the 2 × CO_2 climate the seasonal changes in global lightning frequencies are +31% (DJF), +25% (MAM), +35% (JJA), and +28% (SON). For the −2% S_0 climate the seasonal changes are −24% (DJF), −28% (MAM), −25% (JJA), and −18% (SON).

For the climate change experiments, all months of the year indicate larger percentage changes for cloud-to-ground lightning than for intracloud lightning. From the formulation of the parameterization used to calculate cloud-to-ground lightning [*Price and Rind*, 1993], this implies that as the climate changes, there is a systematic change in the thickness of the

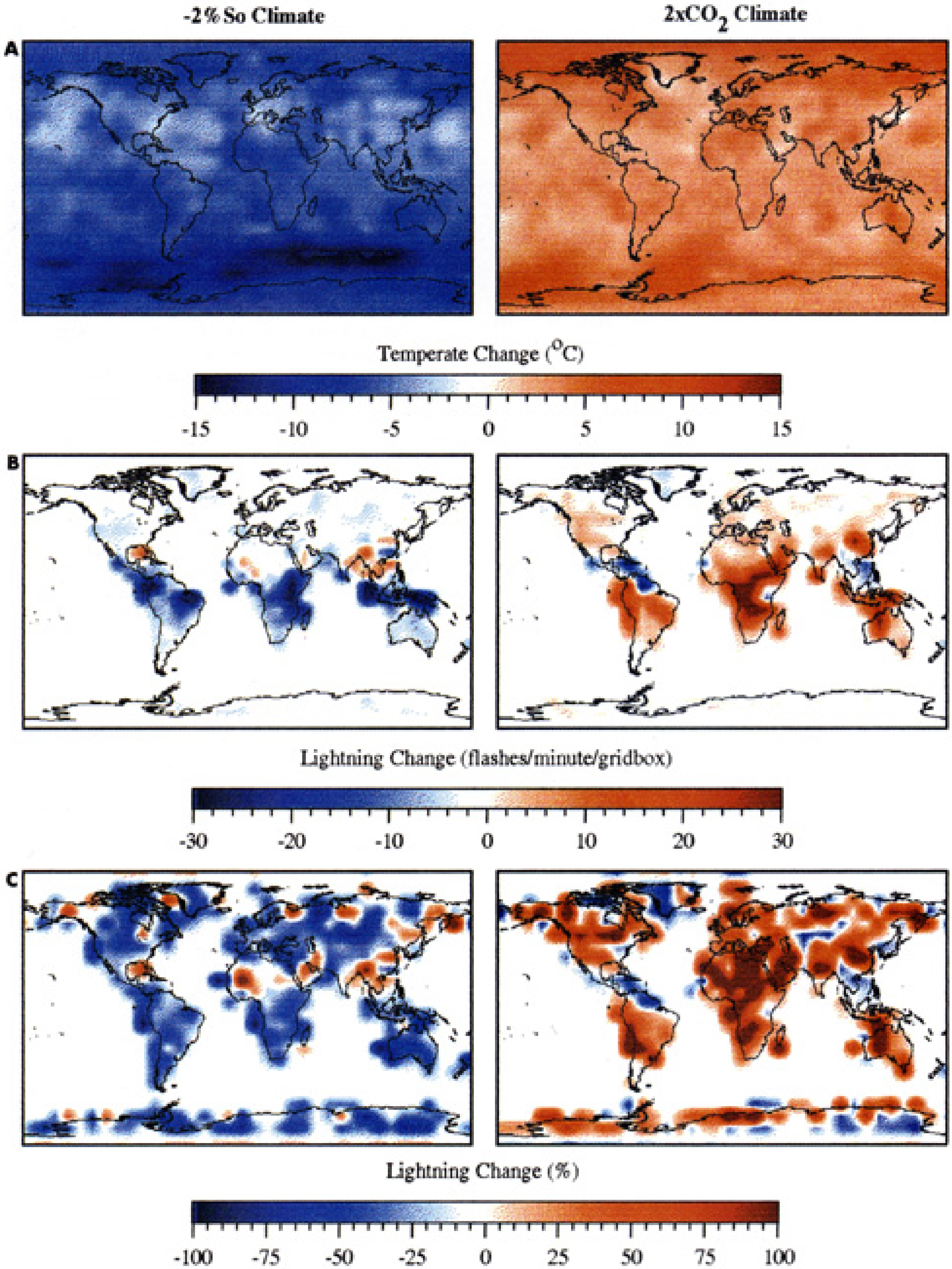

Plate 1. Annual mean (a) surface temperature changes; (b) absolute lightning changes; and (c) percentage changes in lightning frequencies for two climate change scenarios: $2 \times CO_2$ climate (right-hand figures) and a -2% S_0 climate (left-hand figures). Red/blue shading implies increases/decreases in temperature and lightning activity.

cold cloud region in thunderstorms, which is the region of significant charge generation in thunderstorms. Both the depth of the thunderstorms and the height of the freezing level change as climate changes. Since our parameterization relates the thickness of the thunderstorm above the freezing level to the fraction of cloud-to-ground flashes in thunderstorms, these results imply that in a warmer/colder climate the volume of the cold cloud region decreases/increases as a result of larger changes in freezing level height than in total cloud depth. This model result implies a larger/smaller proportion of cloud-to-ground lightning in thunderstorms in warmer/colder climates.

Latitudinal and Longitudinal Changes

The sensitivity of the cold cloud thickness to climate change is further emphasized in Figure 3, where the annual mean latitudinal variations of the fraction of cloud-to-ground lightning in thunderstorms (and hence cold cloud thickness) is shown. The control climate's latitudinal distribution of cold cloud thicknesses is in good agreement with observations [*Price and Rind*, 1993]. The latitudinal gradient of the above parameters in the model appears to be weakened/strengthened in the warmer/colder climates. Whereas the fraction of cloud-to-ground lightning is larger/smaller in the tropics and subtropics for the $2 \times CO_2/-2\%\ S_0$ experiments, the trends appear to be reversed at high latitudes. However, since the majority of lightning occurs in the tropics, the tropical changes dominate the global lightning values (Figure 2).

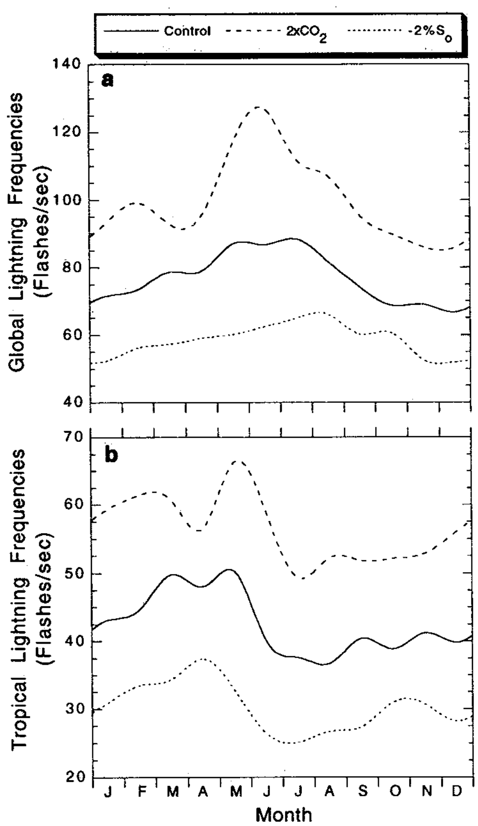

Figure 2. Seasonal distributions of total lightning frequencies in the control climate and the two climate change scenarios for (a) the globe and (b) the tropics.

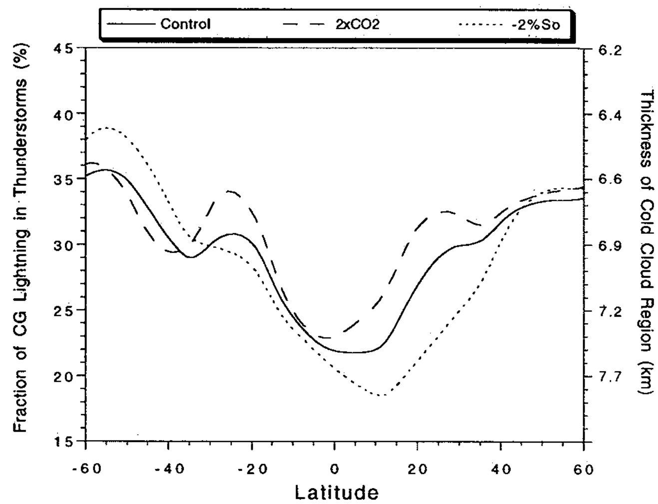

Figure 3. Annual mean latitudinal distribution of the fraction of cloud-to-ground lightning in thunderstorms, derived from the latitudinal variations of the thickness of the cold cloud regions in deep convective clouds. The results for the three climate scenarios are presented.

In the control climate the model produces a large maximum of lightning in the tropics, in agreement with observations [*Turman and Edgar*, 1982]. The annual mean latitudinal changes in lightning activity (total, intracloud, and cloud-to-ground lightning) for both experiments are shown in Figure 4. Increases/decreases in lightning activity for the warm/cold climate occur at most latitudes. In the tropics, where the absolute magnitude of lightning activity is greatest, the cloud-to-ground lightning frequencies are most sensitive to climate changes. For the $2 \times CO_2$ climate the largest increases in lightning occur in the southern hemisphere subtropics, with little changes occurring at high latitudes. However, for the $-2\%\ S_0$ climate, significant decreases in lightning occur at most latitudes, except for a slight increase in intracloud frequencies in the northern hemisphere subtropics.

There are a few possible reasons why lightning frequencies are affected differently at different latitudes. Processes that affect convection differ at different latitudes. In low latitudes a warmer climate results in increased evaporation as well as larger surface temperatures, which results in a more statically unstable atmosphere. This results in more intense air mass thunderstorms. However, in higher latitudes, convection is part of the dynamics of extratropical storms. As the climate warms, high-latitude temperatures increase more than low-latitude temperatures as a result of the snow/ice albedo feedback [*Hansen et al.*, 1984]. This results in a decreased latitudinal temperature gradient which tends to weaken extratropical storms in a warmer climate. Therefore the intensity of convective storms in midlatitudes in a warmer climate depends on the intensity of the midlatitude storm systems themselves. Another latitudinal difference affecting convection in climate change scenarios is large-scale subsidence. Changes in convection in the tropics affect the intensity of subsidence in the subtropics, which can have a large influence on the vertical development of thunderstorms in these regions of subsidence.

In the control run, three longitudinal maxima in lightning

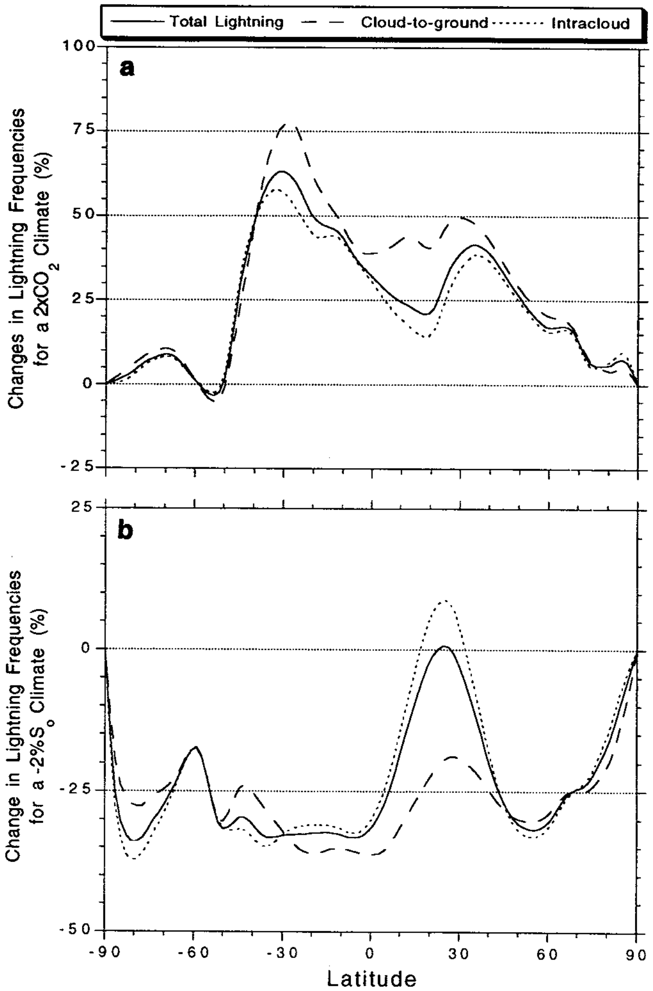

Figure 4. Annual mean latitudinal changes in total, intracloud, and cloud-to-ground lightning frequencies for the two climate change scenarios.

activity are reproduced, associated with the three major tropical land masses [*Price and Rind*, 1994]. The annual mean longitudinal changes in lightning activity are presented in Figure 5. In both experiments, most longitudinal bands show larger changes for cloud-to-ground lightning than for intracloud lightning; however, over the Pacific Ocean (150°E–110°W) the changes in intracloud flashes appear to be dominant. Although the absolute changes over the Pacific are small, the above implies that the volume of these deep convective storms above the freezing level increases/decreases over the Pacific in the warmer/colder climate, whereas the opposite is true in other regions.

Even though there are locations where intracloud lightning and total lightning decrease/increase in a warmer/colder climate, the cloud-to-ground lightning is always enhanced in a warmer atmosphere and always suppressed in a colder atmosphere. In both climate scenarios the largest changes in both intracloud and cloud-to-ground lightning occurs over Africa (0°–50°E), although the magnitude of the changes for the $2 \times CO_2$ climate are twice those for the -2% S_0 climate. These different longitudinal changes in lightning frequencies are strongly influenced by the longitudinal distribution of land and ocean. Since lightning is mainly a continental phenomena, the largest change in lightning activity occurs over the longitudinal band where land is most prevalent. Because little lightning occurs over the oceans, ocean regions contribute little to the total longitudinal change in lightning frequencies. Sea surface temperatures are an additional contributor to longitudinal differences in lightning changes. Cooler sea surface temperatures warm more rapidly than warmer waters, resulting in reduced meridional circulations in a warmer climate. These circulation changes, such as the Walker circulation, can further contribute to longitudinal differences in the lightning frequency changes.

It should be noted that all the above mentioned changes are percentage changes and not absolute changes. The absolute values for lightning in the control run, the reference climate for these experiments, are presented by *Price and Rind* [1994].

Diurnal Changes

Because of computational limitations the diurnal cycle of lightning activity in the GCM is saved for only a few locations (grid boxes). For this study we have chosen two locations: tropical West Africa (5°W, 12°N) and the western United States (105°W, 44°N). The annual mean diurnal

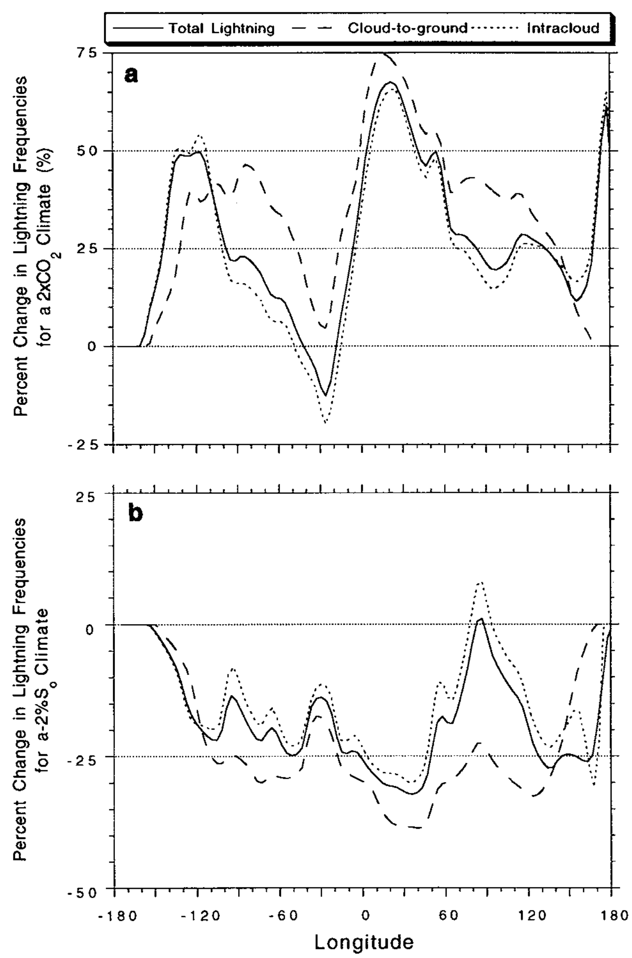

Figure 5. Annual mean longitudinal changes in total, intracloud, and cloud-to-ground lightning frequencies for the two climate change scenarios.

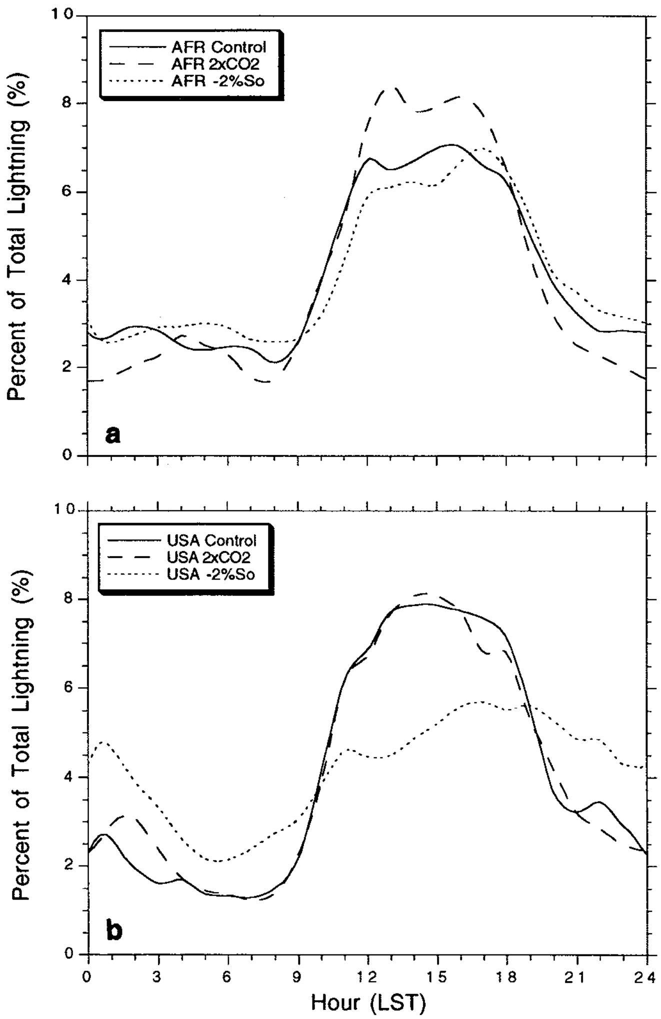

Figure 6. Annual mean diurnal variations of total lightning activity in (a) tropical West Africa and (b) western United States. All three climate scenarios are presented.

variation of total lightning activity for the two climate experiments, together with the control run, are shown in Figure 6.

In both locations the lightning activity in the control climate peaks in the midafternoon with the minimum during the early morning hours, in agreement with observations [*Oladipo and Mornu*, 1985; *Reap*, 1986]. By changing the climate, the phase of the diurnal cycle does not vary significantly. However, the amplitude of the diurnal signal does change. The warmer/colder climate appears to amplify/reduce the diurnal signal. In the case of the United States (Figure 5b) the amplification is only slight (9%) for the warmer climate; however, for the colder climate the diurnal amplitude is dramatically reduced (−64%).

Conclusions and Discussion

The Goddard Institute for Space Studies general circulation model has been used to investigate the possible implications of global climate change on global lightning distributions. Both intracloud and cloud-to-ground lightning frequencies are simulated using parameterizations that involve convective cloud parameters. These parameters are determined using a penetrative convective scheme. Lightning diagnostics are available at spatial scales from global down to individual grid boxes (500- to 1000-km resolution) and at temporal scales from annual down to diurnal.

Two climate scenarios were considered. The first for an atmosphere with twice today's concentrations of CO_2 (representing a 4.2°C global warming) and the second for a climate where the solar output is reduced by 2% (representing a 5.9°C global cooling).

The results suggest an increase/decrease in global lightning activity of approximately 5–6% for every 1°C increase/decrease in global surface temperatures. For the $2 \times CO_2$/-2% S_0 climate a 30% increase/24% decrease in global lightning activity occurs. Changes in lightning activity appear to be largest during northern hemisphere summer (JJA) for the warmer climate and during northern hemisphere spring (MAM) for the colder climate. These seasonal changes tend to reduce to amplitude of the tropical semiannual cycle of lightning activity as the climate warms. However, the global annual cycle appears to be intensified in a warmer climate.

The largest changes in lightning activity occur over continental regions, with Africa dominating in both climate scenarios. Cloud-to-ground lightning frequencies, although only 25% of the total lightning in the control experiment, appear to be more sensitive to climate change than intracloud lightning frequencies. This appears to be due to changes in the thickness of the mixed phase region in the model's convective clouds as climate changes.

In addition, the model's results suggest that diurnal variations in lightning activity tend to become more amplified as the climate warms, although the phase of the diurnal fluctuations remains fairly constant.

The above results imply that global lightning activity has a much weaker sensitivity to temperature change than found by *Williams* [1992]. Williams compared Schumann resonance to tropical land temperatures. The results showed that during El Niño years, when the tropics are anomalously warm, the Schumann resonance increases by fourfold for every 1°C increase in temperature. There are a few possible explanations as to why such large discrepancies exist. First, only tropical land temperatures are used in the *Williams* [1992] paper, whereas this study considers global land and ocean temperatures. Since the global lightning signal originates over tropical landmasses, the sensitivity of lightning frequencies to changes in tropical land temperatures will be much larger than for global land and ocean temperatures combined. *Price* [1993] recently showed that when global land and ocean temperatures are compared to a global lightning index, the sensitivity of lightning activity to surface temperature changes is similar to that presented in this study. Second, El Niño years result in changes in oceanic and atmospheric circulations which result in shifts in convection. These changes in atmospheric patterns as a result of El Niño warming differ from those patterns expected as a result of global warming from increased levels of trace gases in the atmosphere. Changes in deep convection patterns as a result of El Niño cannot presently be modeled in GCMs. Third, because of the coarse resolution of present GCMs it is possible that the sensitivity of lightning activity to temperature change may increase as model resolution increases. This will have to be addressed in future studies.

The results of this study will likely depend on the moist convective scheme utilized in GCMs as well as the magnitude and distribution of the induced climate changes. A large portion of the induced climate change is a result of cloud feedback processes in the GCM. For the doubled CO_2 climate, cloud feedbacks alone result in approximately a 1°C warming, 25% of the total warming [*Hansen et al.*, 1984]. The positive cloud feedbacks in the warmer climate result from a small increase in mean cloud height as well as a small decrease in the total cloud cover. The major increase in cloud height is due to increases in high-level cirrus clouds at low latitudes, consistent with the increase of penetrating moist convection at those latitudes. Since clouds absorb thermal infrared radiation, the higher the cloud the cooler is its radiating temperature. Therefore increasing cloud height implies weaker infrared emission to space and a positive feedback in a warming climate. The reduced cloud cover in the warmer climate primarily represents the reduction of low- and middle-level clouds, due to changes such as enhanced subsidence as a result of increased vertical transport of moisture by convection and the large-scale dynamics and decreases in eddy energy (midlatitude storms) from the reduced latitudinal temperature gradient. Reductions in the cloud amount imply more shortwave solar radiation reaching the Earth's surface, resulting in a further positive feedback in a warmer climate.

In addition to the cloud feedbacks, water vapor feedbacks play a major role in the global temperature changes, with the change in vertical distribution of water vapor accounting for approximately 1°C warming. These feedbacks are dominant in tropical regions where the majority of thunderstorms occur and depend on the cloud and convection scheme used. Our ability to model cloud processes in GCMs is still very limited, since many of the crucial cloud processes occur on small scales, and have to be parameterized in global models. Moreover, inadequate observations and poor understanding of certain cloud processes add to the uncertainties in our results. Similarly, details of convection schemes are equally poorly constrained by observations. Therefore different cloud and convection parameterizations in different models may provide different results regarding lightning frequencies as climate changes. It is therefore possible that our results could be either overestimating or underestimating the changes in lightning frequency that may occur as a result of any future global warming.

With due consideration of the caveats involved in this study, the results indicate that if our climate warms as projected due to increases in trace gas concentrations in our atmosphere, significant increases in lightning frequency should become apparent. This is in agreement with recent observations relating observed surface temperature fluctuations to indexes of global lightning activity [*Williams*, 1992; *Price*, 1993]. The implications of these findings are widespread.

For tropospheric chemistry, lightning is a major source of NO_x. NO_x in turn affects the concentration of ozone in the atmosphere, which is a greenhouse gas. Furthermore, changes in the ratio of intracloud to cloud-to-ground discharges as well as increases in the depth of penetrating convection in a warmer climate can result in changes in the vertical distribution of NO_x in the atmosphere, which could have major consequences on tropospheric chemistry.

Natural forest fires are ignited by lightning and may therefore increase in frequency in a warmer climate. In addition to fire frequency, drought conditions are expected to increase in a warmer climate [*Rind et al.*, 1990], possibly resulting in more intense fires in the future. To verify this hypothesis, it may be possible to use paleoclimatic data to study past fire regimes in geological records, lake sediments, and tree rings. Studies of this type do show enhanced natural fire frequencies and intensities during warmer climatic periods in our past [*Winkler*, 1985; *Clark*, 1988]. Further paleoclimate studies could help verify the model's sensitivity to climate perturbations.

The social implications of this study may also be dramatic. Presently, more than 100 people are killed by lightning every year in the United States alone, more deaths than by tornados, hurricanes, or floods. Electrical power companies lose millions of dollars every year from replacing transformers and power lines that are damaged by electrical surges caused by lightning [*Clary and Wood*, 1985]. In addition, aircraft and spacecraft are also extremely vulnerable to lightning discharges [*Uman and Krider*, 1989]. Increases in the frequency of lightning activity of the magnitude projected here would have major ramifications for all the above lightning-related phenomena.

Acknowledgments. Climate modeling at GISS is supported by the NASA Climate Program Office as well as the United States Environmental Protection Agency offices of Policy Analysis and Research and Development. The help of Rick Healy in running the climate simulations is greatly appreciated.

References

Buechler, D. E., P. D. Wright, and S. J. Goodman, Lightning/rainfall relationships during COHMEX, in *Proceedings of the 16th Conference on Severe Storms and Conference on Atmospheric Electricity*, American Meteorological Society, Boston, Mass., 1990.

Clark, J. S., Effect of climate change on fire regimes in northwestern Minnesota, *Nature*, *334*, 233–235, 1988.

Clary, M., and R. A. Wood, Lightning! Spectacular and deadly, *Weatherwise*, *38*(3), 128–151, 1985.

DelGenio, A. D., and K. B. McGrattan, Moist convection and the vertical structure and water abundance of Jupiter's atmosphere, *Icarus*, *84*, 29–53, 1990.

Franzblau, E., and C. J. Popp, Nitrogen oxides produced from lightning, *J. Geophys. Res.*, *94*, 11,089–11,104, 1989.

Hansen, J., G. Russell, D. Rind, P. Stone, A. Lacis, S. Lebedeff, R. Reudy, and L. Travis, Efficient three-dimensional global models for climate studies: Models I and II, *Mon. Weather Rev.*, *111*, 609–662, 1983.

Hansen, J., A. Lacis, D. Rind, G. Russel, P. Stone, I. Fung, R. Reudy, and J. Lerner, Climate sensitivity: Analysis of feedback mechanisms, in *Climate Processes and Climate Sensitivity*, *Geophys. Monogr. Ser.*, vol. 29, edited by J. E. Hansen and T. Takahashi, pp. 130–162, AGU, Washington, D. C., 1984.

Intergovernmental Panel on Climate Change (IPCC), *The IPCC Scientific Assessment*, edited by J. T. Houghton, G. J. Jenkins, and J. J. Ephraums, Cambridge University Press, New York, 1990.

Jacobson, E. A., and E. P. Krider, Electrostatic field changes produced by Florida lightning, *J. Atmos. Sci.*, *33*, 103–114, 1976.

Jorgensen, J. M., and M. A. LeMone, Vertical velocity characteristics of oceanic convection, *J. Atmos. Sci.*, *46*, 621–640, 1989.

Krumm, H. C., Der weltzeitliche Tagesgang der Gewitterhaufigkeit, *Z. Geophys.*, *28*, 85–104, 1962.

Lhermitte, R., and E. R. Williams, Cloud electrification, *Rev. Geophys.*, *21*, 984–992, 1983.

Livingston, J. M., and E. P. Krider, Electric fields produced by Florida thunderstorms, *J. Geophys. Res.*, *83*, 385–401, 1978.

Oladipo, E. O., and M. E. Mornu, Characteristics of thunderstorms in Zaria, Nigeria, *Weather*, *40*, 316–322, 1985.

Price, C., Global surface temperatures and the earth's electric circuit, *Geophys. Res. Lett.*, *20*, 1363–1366, 1993.

Price, C., and D. Rind, A simple lightning parameterization for calculating global lightning distributions, *J. Geophys. Res.*, *97*, 9919–9933, 1992.

Price, C., and D. Rind, What determines the cloud-to-ground lightning fraction in thunderstorms? *Geophys. Res. Lett.*, *20*, 463–466, 1993.

Price, C., and D. Rind, Modeling global lightning distributions in a general circulation model, *Mon. Weather Rev.*, in press, 1994.

Reap, R. M., Evaluation of cloud-to-ground lightning data from the western United States for the 1983–84 summer seasons, *J. Clim. Appl. Meteorol.*, *25*, 785–799, 1986.

Rind, D., R. Goldberg, J. Hansen, C. Rosensweig, and R. Reudy, Potential evapotranspiration and the likelihood of future drought, *J. Geophys. Res.*, *95*, 9983–10,004, 1990.

Rust, W. D., and R. J. Doviak, Radar research on thunderstorms and lightning, *Nature*, *297*, 461–468, 1982.

Rutledge, S. A., E. R. Williams, and T. D. Keenan, The Down Under Doppler and Electricity Experiment (DUNDEE): Overview and preliminary results, *Bull. Am. Meteorol. Soc.*, *73*, 3–16, 1992.

Saunders, C. P. R., W. D. Keith, and R. P. Mitzeva, The effect of liquid water on thunderstorm charging, *J. Geophys. Res.*, *96*, 11,007–11,017, 1991.

Shackford, C. R., Radar indications of a precipitation-lightning relationship in New England thunderstorms, *J. Meteorol.*, *17*, 15–19, 1960.

Takahashi, T., Near absence of lightning in torrential rainfall producing Micronesian thunderstorms, *Geophys. Res. Lett.*, *17*, 2381–2384, 1990.

Trent, E. M., and S. G. Gathman, Oceanic thunderstorms, *Pure Appl. Geophys.*, *100*, 60–69, 1972.

Turman, B. N., and B. C. Edgar, Global lightning distributions at dawn and dusk, *J. Geophys. Res.*, *87*, 1191–1206, 1982.

Uman, M. A., and E. P. Krider, Natural and artificially initiated lightning, *Science*, *246*, 457–464, 1989.

USDA Forest Service, *1984–1990 Wildfire Statistics*, State and Private Forestry, Fire and Aviation Management Staff, Washington, D. C., 1992.

Williams, E. R., Thunderstorm electrification: Precipitation versus convection, PhD. thesis, MIT, Cambridge, Mass., 1981.

Williams, E. R., Large-scale charge separation in thunderclouds, *J. Geophys. Res.*, *90*, 6013–6025, 1985.

Williams, E. R., Schumann resonance: A global tropical thermometer, *Science*, *256*, 1184–1187, 1992.

Williams, E. R., Global circuit response to seasonal variations in global surface air temperatures, *Mon. Weather Rev.*, in press, 1994.

Williams, E. R., M. E. Weber, and R. E. Orville, The relationship between lightning type and convective state of thunderclouds, *J. Geophys. Res.*, *94*, 13,213–13,220, 1989.

Winkler, M. G., A 12,000-year history of vegetation and climate for Cape Cod, Massachusetts, *Quart. Res.*, *23*, 301–312, 1985.

C. Price, Global Climate Research Division, Lawrence Livermore National Laboratory, P.O. Box 808, Livermore, CA 94551.

D. Rind, NASA Goddard Institute for Space Studies, 2880 Broadway, New York, NY 10025.

(Received December 31, 1992; revised December 9, 1993; accepted December 27, 1993.)